Geomechanics and Engineering, *Vol. 39, No. 3 (2024) 317-331*
https://doi.org/10.12989/gae.2024.39.3.317

Effect of different groundwater levels on seismic response of subway stations shallowly buried in the sand foundation

Min-Zhe Xu, Zhen-Dong Cui* and Li Yuan

State Key Laboratory of Intelligent Construction and Healthy Operation & Maintenance of Deep Underground Engineering, School of Mechanics and Civil Engineering, China University of Mining and Technology, Xuzhou, Jiangsu, 221116, P.R. China

(*Received January 31, 2024, Revised October 16, 2024, Accepted October 22, 2024*)

Abstract. Sand liquefaction caused by earthquakes is one of the serious threats to underground stations. The change in groundwater level may have a great influence on the seismic behavior of underground stations buried in sand foundations. In this paper, a 3D numerical model for the soil-structure interaction system was established by applying the fully nonlinear finite difference program FLAC^{3D}. The impact of different groundwater levels on the seismic behavior of underground stations was explored in numerical analyses. The fluid-solid coupling and different seismic intensities were taken into consideration in the model. The numerical results demonstrate that the decrease of groundwater level significantly restrains the uplift of the underground station and the liquefaction of the site. The dynamic soil pressure around the sidewall under a higher water table is larger than that under a low water table. Under the earthquake, the ground peak acceleration increases as the groundwater level decreases. For the station structure, the decrease of groundwater level is unfavorable to the shear resistance of the middle columns. However, the effect of different groundwater levels on the axial stress of the middle columns is relatively small. The research results can be used as a reference for the seismic design of subway stations shallowly buried in the sand foundation with different groundwater levels.

Keywords: groundwater level; sand liquefaction; seismic response; soil-structure interaction; subway station

1. Introduction

Ground deformation caused by sand liquefaction is one of the most serious threats to the safety of buildings and infrastructures. In the past, underground structures have suffered severe damage due to sand liquefaction (Tokimatsu and Asaka 1998, Kang *et al.* 2014). For example, there was widespread sand liquefaction during the 1964 Niigata earthquake, which led to serious damage of a lot of underground pipelines (Hamada *et al.* 1987). Meanwhile, sand liquefaction resulting in the damage of underground structures was also detected in some other seismic events, such as the 1993 Kushiro-Oki earthquake (Suzuki *et al.* 2006), the 1994 Hokkaido Toho-Oki earthquake (Koseki *et al.* 2000) and the 1995 Kobe earthquake (Zhuang *et al.* 2015a). With the rapid development and increasingly serious traffic congestion in China, a lot of subway stations have been built in recent years and many of them are buried in the sand foundation. Sand liquefaction can have a serious influence on the seismic behavior of subway stations. Thus, subway stations buried in the sand foundation are at great risk of seismic damage.

In the past, given the constraints of the soil and rock, underground structures were usually considered to have greater seismic performance than ground structures (Lu and Hwang 2019). Since the Kobe earthquake in 1995, the complete failure of the Daikai station has attracted widespread attention to the seismic defense of underground buildings all over the world. To inquire about the seismic performance of underground structures, plenty of numerical research has been carried out in recent years (Hashash *et al.* 2001, Dong *et al.* 2020, Kwon *et al.* 2020, Sudevan *et al.* 2020, Ebadi-Jamkhaneh *et al.* 2021, Cui *et al.* 2023a, Jaber *et al.* 2023). The research results demonstrated that the middle columns are the parts of subway stations that are most susceptible to seismic damage. Compared to the deeply buried underground structure, the shallowly buried structure is more likely to be destroyed in earthquakes (Unutmaz 2014, Cheng and Sun 2018). Ground deformation also greatly affects the seismic behavior of subway stations (Huo *et al.* 2005). Therefore, subway stations shallowly buried in the sandy soil foundation may suffer more serious seismic damage due to ground deformation induced by sand liquefaction. In liquefiable sites, soil liquefaction may lead to the uplift of underground structures, which will further cause large ground displacement (Sudevan *et al.* 2020, Chou and Lin 2020). The site close to the subway station is more likely to liquefy than the site further away and the seismic behavior of underground stations may be weakened by the liquefied soils. (Zhuang *et al.* 2015a). The uplift behavior of subway stations aggravates the liquefaction degree of the foundation below the station (Wang *et al.* 2019). Meanwhile, seismic intensity plays a critical role in the study of seismic response. The seismic response of subway stations was commonly studied by applying different seismic intensities (Tsinidis 2017, Yoo *et al.* 2022, Xu *et al.* 2024). The degree of sand liquefaction is usually

*Corresponding author, Professor
E-mail: cuizhendong@cumt.edu.cn

ISSN: 2005-307X (Print), 2092-6219 (Online)

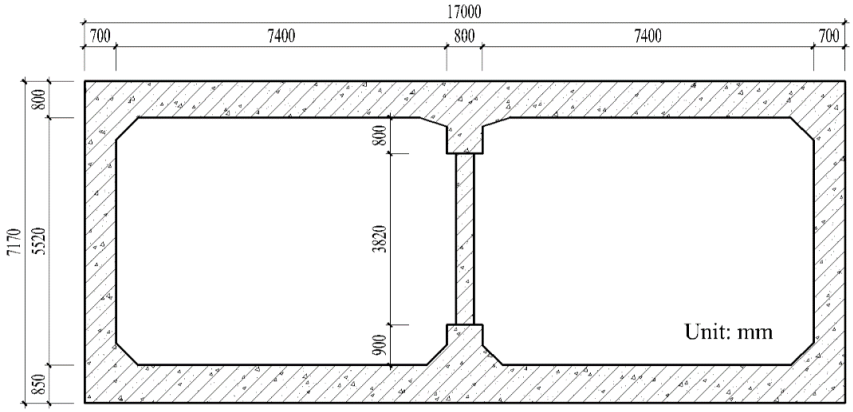

Fig. 1 Cross-section of the Daikai station

higher under strong earthquakes than under relatively weak earthquakes (Azadi and Hosseini 2010). The increment of the PGA of seismic waves leads to a more obvious phenomenon of high-frequency filtering and low-frequency amplification (Chen *et al.* 2014). Currently, most of the research focuses on the seismic defense of underground stations shallowly buried in fully saturated sand foundations. However, few studies concentrate on the impact of different groundwater levels on the seismic behavior of underground stations buried in the sand foundation. In natural soil layers, the groundwater level is not necessarily at the ground surface. Thus, it is vital to explore the seismic behavior of underground stations and the surrounding sites with different groundwater levels.

Herein, the effects of different groundwater levels on the seismic behavior of the Daikai subway station were investigated by numerical analyses in this paper. A 3D numerical model for the dynamic interaction soil-structure system was established by applying the fully nonlinear finite difference program FLAC^{3D}. The fluid-solid coupling was considered in the numerical calculation model. Meanwhile, the impact of input ground motions with different seismic intensities on the seismic behavior of the subway station and the surrounding soil was explored. According to the numerical results, the effects of groundwater level on the site liquefaction, ground displacement, dynamic soil pressure, ground acceleration and structural stress were discussed and analyzed, respectively.

2. Numerical models

2.1 Soil and station models

The Daikai station was the first underground station to be destroyed by an earthquake, which has attracted widespread attention to the seismic behavior of underground stations. The construction of the Daikai station used the cut-and-cover method and the impacts of earthquakes were not considered in the structural design (Iida *et al.* 1996). The failure of the Daikai station led to a maximum settlement of 2.5 m on the ground surface in the 1995 Kobe earthquake (Sun *et al.* 2019). Therefore, the most seriously damaged part of the Daikai station was used as the numerical station model. The cross-section size of the selected part was 17 m in width and 7.17 m in height, as shown in Fig. 1. The middle columns were 3.82 m high and were supported by the 1.6 m high upper beam and the 1.75 m high lower beam. The middle column has a rectangular cross-section with a size of 1.0 m×0.4 m. The longitudinal distance between the middle columns was 3.5 m. The Daikai station was buried around 4.8 m under the surface.

A three-dimensional numerical model with the size of 119 m×10.5 m×30 m was established by the finite difference program FLAC^{3D}, consisting of the Daikai station and the surrounding sand foundation, as illustrated in Fig. 2(a). The three spans in the longitudinal direction of the subway station were selected, as seen in Fig. 2(b). The calculation model has 13441 solid elements and 17217 grid nodes. The monitoring plane was located in the center of the longitudinal direction of the model. To explore the effect of groundwater level, four different depths of the water table were considered, as depicted in Fig. 3. The depth of the groundwater level (H) was determined to be the distance between the ground surface and the groundwater surface. The fluid-solid coupling was considered in the calculation model.

In the numerical analyses, the application of the boundary conditions was divided into two steps. In the static analysis step, the normal displacement constraints were applied on the bottom boundary and lateral boundary by fixing the nodal velocity of the boundaries. Subsequently, the lateral boundary condition was released in the dynamic calculation step. The normal displacement on the model bottom boundary was constrained considering that the numerical model was positioned on the bedrock surface. The free-field boundary was adapted to the lateral boundary to mitigate the effect of the reflected wave. The seismic waves were applied by setting the acceleration time history at the bottom boundary.

The maximum calculation element size was determined to satisfy seismic wave propagation calculation accuracy requirements, which was expressed as Eq. (1) (Kuhlemeyer and Lysmer 1973).

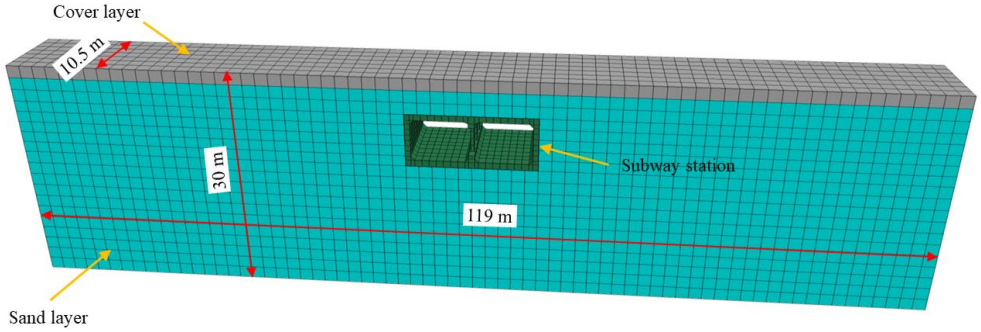

(a) 3D FDM model for the soil-structure interaction system

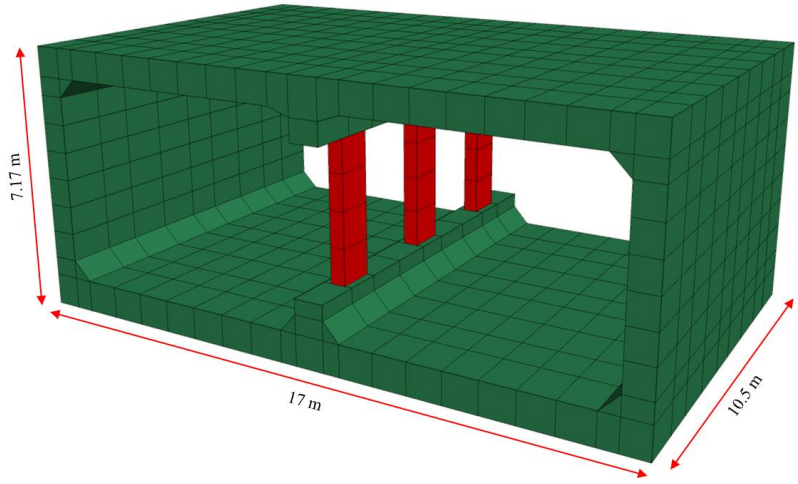

(b) 3D FDM model of the subway station

Fig. 2 Numerical model for soil and subway station

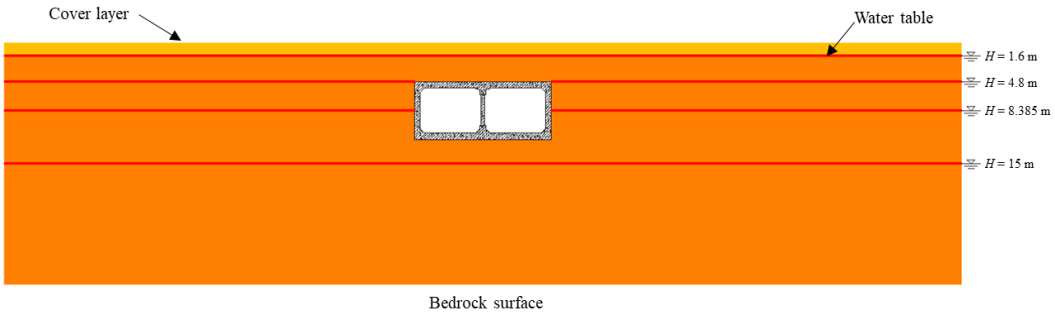

Fig. 3 Depths of the groundwater level

$$\Delta Z_{max}\left(\frac{1}{8}\sim\frac{1}{10}\right)\frac{V_s}{f_{max}} \quad (1)$$

where V_s is the velocity of the shear wave; f_{max} is the cut-off frequency of the seismic wave, taken as 5 Hz. Therefore, the maximum element size adopted in this study was 1.7 m.

For the soil-structure contact relationship, the slip and separation of the contact surface were described by using the no-thickness surface element. The contact surface consists of a large number of triangular surface elements with three nodes, as shown in Fig. 4. The contact surface nodes are generated if the contact surface and target surface connect. Each node has a corresponding representation area.

The contact stiffness in the tangential and normal directions was determined to be ten times the corresponding stiffness of the underground station (Wu *et al.* 2021). The contact surface follows the Coulomb friction criterion in the tangential direction. The friction angle and cohesion of the contact surface were determined to be 21.8° ($\mu = 0.4$) (Bobet *et al.* 2008, Cui *et al.* 2023b) and 0, respectively.

2.2 Constitutive model and material properties

In the dynamic calculation, the Finn constitutive model is usually used to reflect the accumulation of pore water pressure in sand, which is shown in Eq. (2).

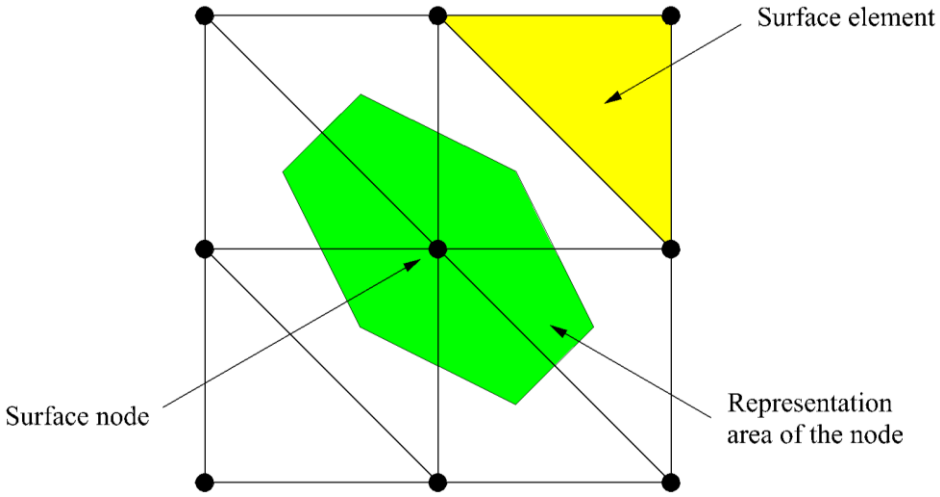

Fig. 4 Contact surface element

Table 1 Numerical calculation parameters of the sand

Parameter	Value	Parameter	Value
Bulk modulus (MPa)	120	Permeability coefficient (cm/s)	1.25×10^{-2}
Shear modulus (MPa)	40	Porosity	0.45
Cohesion (kPa)	0		$C_1 = 0.4299$
Friction angle (°)	35	Byrne model	$C_2 = 0.9304$
Dry density (kg/m^3)	1900		$C_3 = 0$

$$\frac{\Delta\varepsilon_{\mathrm{vd}}}{\gamma} = C_1 \exp\left(-C_2 \frac{\varepsilon_{\mathrm{vd}}}{\gamma}\right) \tag{2}$$

where $\Delta\varepsilon_{\mathrm{vd}}$ is the increment of plastic volume strain; $\varepsilon_{\mathrm{vd}}$ is the plastic volume strain; γ is the shear strain; C_1 and C_2 are the constants.

The detailed numerical calculation parameters of the sand are listed in Table 1. The material of the subway station was C30 concrete, which was assumed to be impervious to water. The concrete in the numerical model was considered to be a linear elastic material. The numerical parameters of the concrete were a density of 2450 kg/m^3, Poisson's ratio of 0.2 and Young's modulus of 30 GPa. The Rayleigh damping was a common and effective damping to model the viscous damping in numerical research. It was regarded as a calculation function of a mass matrix and a stiffness matrix, calculated as Eq. (3).

$$C = \alpha M + \beta K \tag{3}$$

where α and β are the constants of Rayleigh damping; C, M and K are the damping, mass matrix and stiffness matrix of soil. In this study, the Rayleigh damping was applied to the site and the subway station with a critical damping of 2% and 5% respectively. To reduce the influence of the frequency-dependent, the central frequency of the Rayleigh damping was determined by selecting the fundamental frequency of the site and three times the fundamental frequency of the site.

2.3 Seismic input

The seismic waves next to the Daikai station recorded at the Kobe meteorological observatory in the Great Hanshin earthquake were used in this study. Fig. 5 shows the acceleration and the Fourier spectrum of the earthquake. The 1~21 s of the prototype seismic records was taken as the seismic input of the bedrock, which includes the intense ground motion duration. To eliminate the impact of the high-frequency noise, the records were processed by filtering the waves with frequencies larger than 5 Hz. The baseline correction was used to reduce residual velocity and displacement of the model at the end of the dynamic calculation. The peak ground acceleration (PGA) of the records was scaled to 0.1 g, 0.2 g, 0.3 g and 0.4 g respectively to simulate different seismic intensities.

3. Numerical results and analysis for the site

3.1 Site liquefaction

The effect of different groundwater levels on the liquefaction region of the foundation near the station structure during the earthquake with PGA = 0.2 g has been presented, as seen in Fig. 6. The liquefaction is commonly described by the excess pore water pressure (EPWP) ratio, which can be calculated by Eq. (4).

$$R_{\mathrm{u}} = \frac{\Delta u}{\sigma'_{\mathrm{v0}}} \tag{4}$$

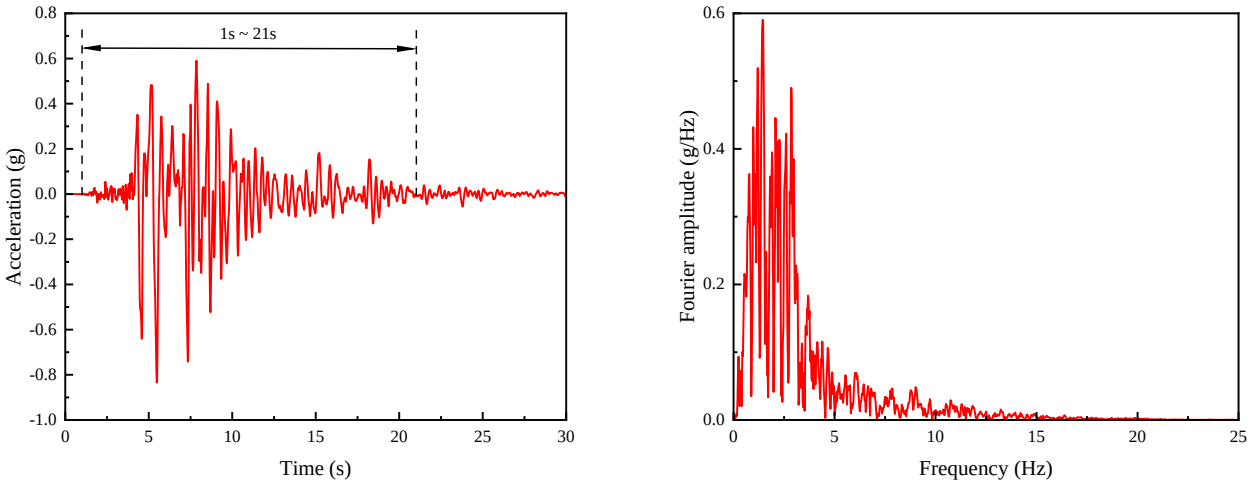

(a) Acceleration (b) Fourier spectrum

Fig. 5 Kobe earthquake record

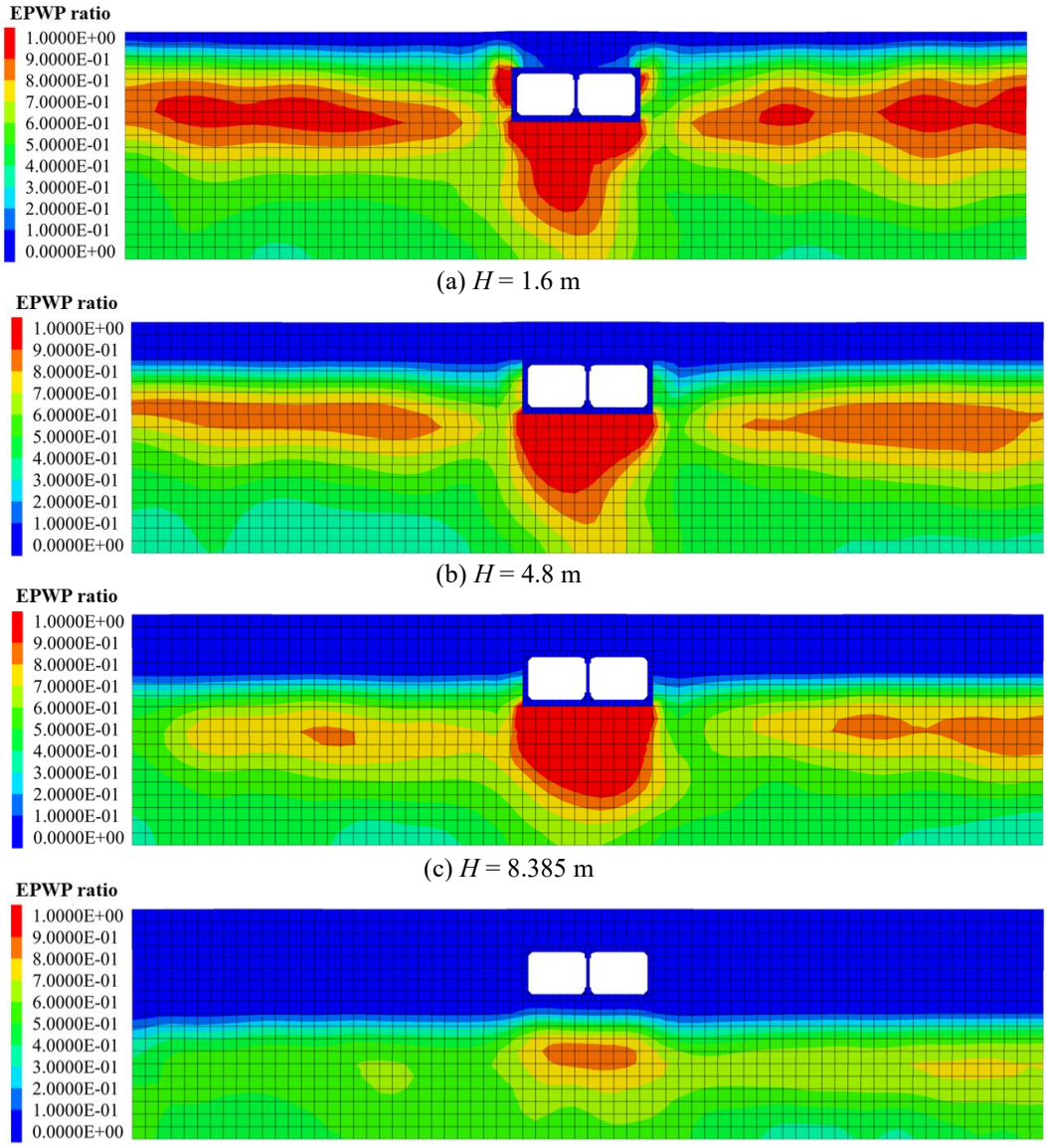

(a) H = 1.6 m

(b) H = 4.8 m

(c) H = 8.385 m

(d) H = 15 m

Fig. 6 Liquefaction region of the site during the earthquake with PGA = 0.2 g

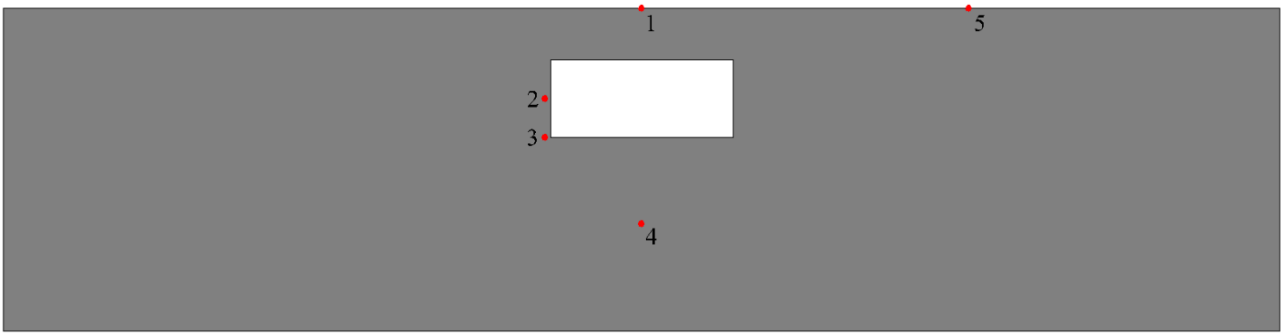

Fig. 7 Measurement points of the site

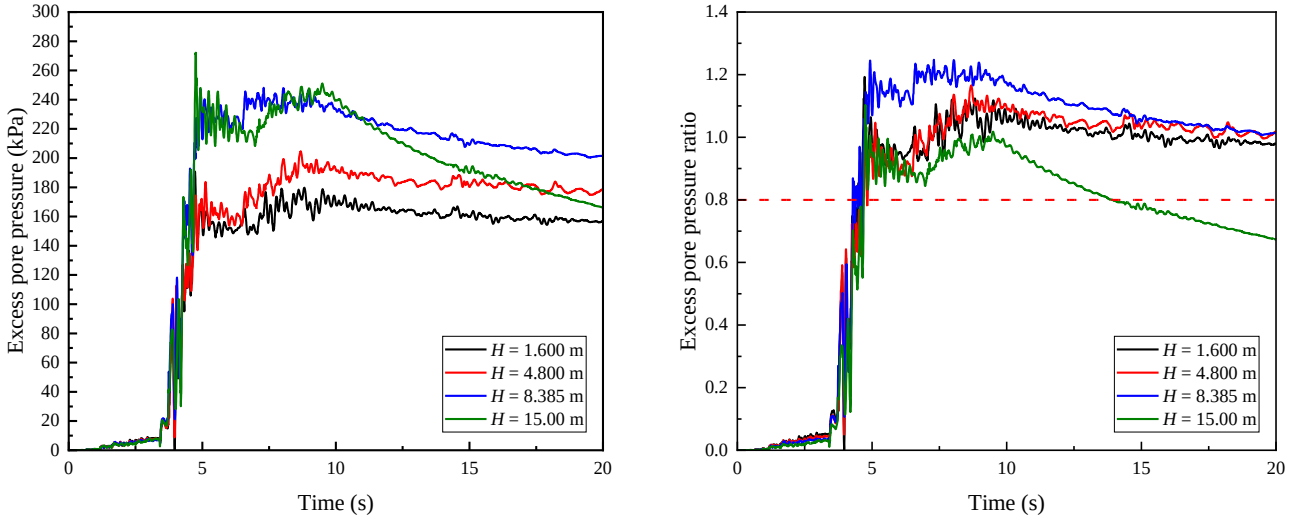

(a) EPWP (b) EPWP ratio

Fig. 8 Dynamic excess pore pressure responses at measurement point 4 under PGA = 0.2 g

where R_u is the EPWP ratio; Δu is the EPWP; σ'_{v0} is the vertical initial effective stress. The sand is generally regarded to be liquefied if the EPWP ratio exceeds 0.8 (Ding *et al.* 2021). It can be shown that the liquefaction of the ground is obviously influenced by the underground station. The liquefaction of the surrounding foundation is restrained by the station structure, which causes no obvious liquefaction around the sidewalls of the subway station. As for the inhibition of the structure on sand liquefaction, some similar conclusions were drawn in a recent study (An *et al.* 2021). Besides, obvious liquefaction behavior has been observed in the site beneath the subway station and the far-field foundation. When the depths of the water table are 1.6 m, 4.8 m and 8.385 m, the depths of soil liquefaction below the station structure are 26.8 m, 26.2 m and 25.5 m, respectively. The liquefaction depth beneath the underground station structure declines with the decrease of the water table. When the depth of the groundwater level is 15 m, only slight liquefaction has been observed in the site below the subway station. There is no obvious liquefaction in the far-field foundation. It can be concluded that the decrease of groundwater level can significantly reduce the liquefaction range of the foundation near the station. The site beneath the station is more likely to liquefy compared to other locations of the foundation. The reason could be that the uplift behavior of the station causes the rise of the EPWP ratio in this area, which agrees with some previous numerical research results for the seismic analysis of the underground station buried in the liquefiable foundation (Wang *et al.* 2019).

The measurement point layout of the site is depicted in Fig. 7. To further explore the impact of different groundwater levels on the liquefaction situation of the foundation with the station, the dynamic EPWP responses of the site under the structure (measurement point 4) subject to the earthquake with PGA of 0.2 g is presented in Fig. 8. In general, the EPWP becomes higher with the water table becoming deeper. After 10 seconds, the dissipation of EPWP when H = 15 m is more significant compared to other groundwater levels. Under the earthquake, the EPWP ratios at the site below the subway station exceed 0.8 under four different groundwater levels, which implies that the soil beneath the structure has undergone liquefaction. In addition, the EPWP ratio rises first and then declines as the depth of the water table increases. The reason for the rise of the EPWP ratio could be that the EPWP grows obviously as the depth of groundwater level rises from 1.6 m to 8.385 m. However, when H = 15 m, the increase in the vertical initial effective stress is larger than the rise of the EPWP, which causes the reduction of the EPWP ratio at measurement point 4.

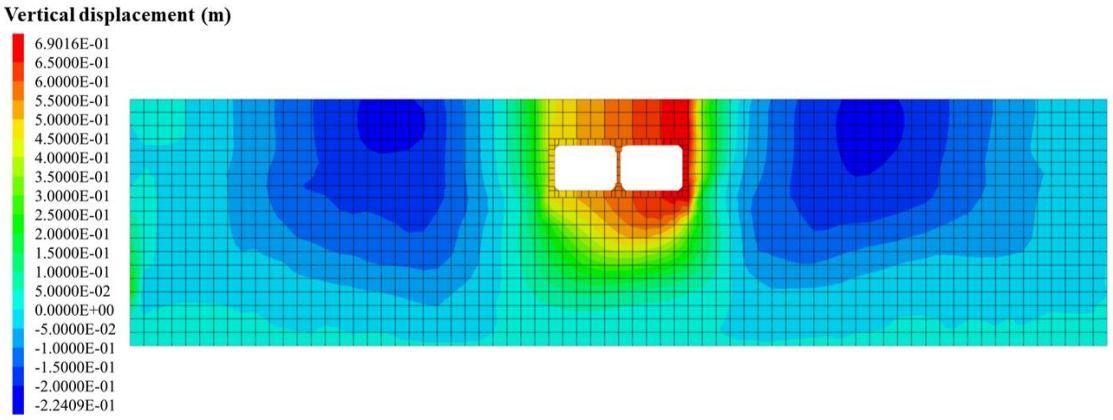

(a) H = 1.6 m

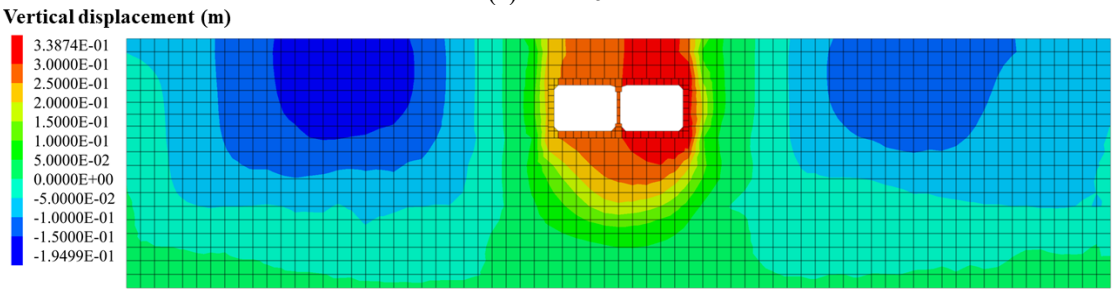

(b) H = 4.8 m

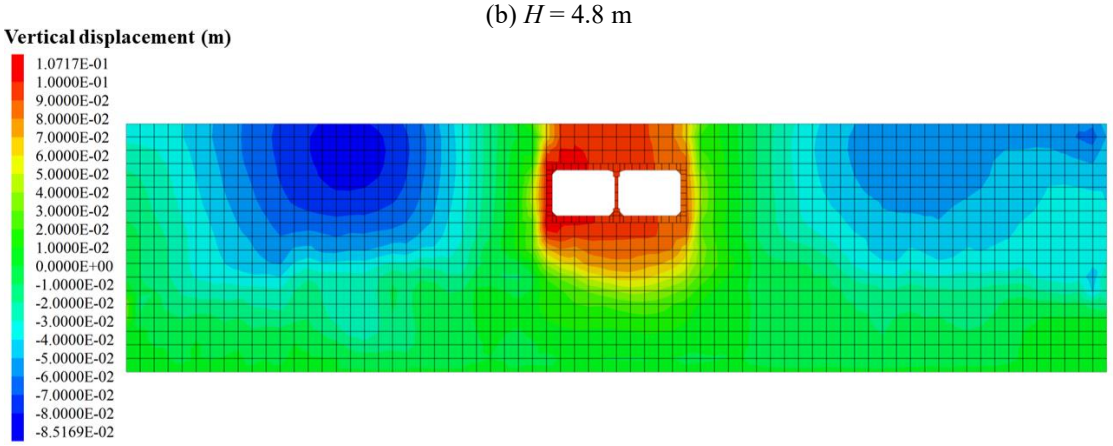

(c) H = 8.385 m

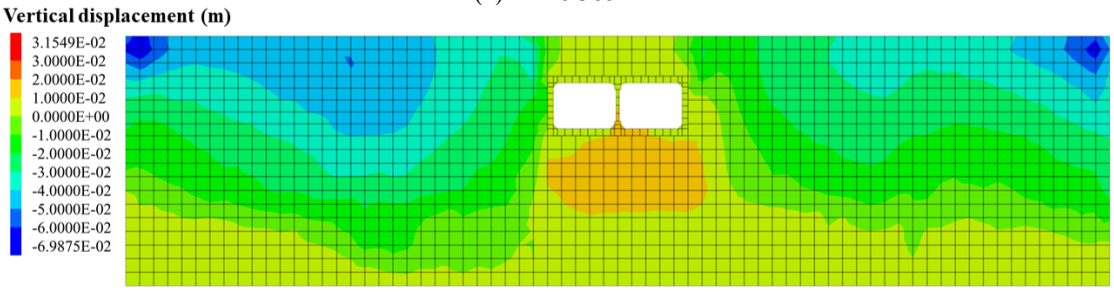

(d) H = 15 m

Fig. 9 Vertical displacement of the overall site under PGA of 0.4 g

3.2 Ground displacement response

The ground displacements for different depths of the water table are then discussed and analyzed. The vertical displacements of the overall site with different groundwater levels under PGA = 0.4 g are presented in Fig. 9. As the depth of the groundwater level increases, the area of ground settlement adjacent to the station structure gradually decreases. The subway station buried in the foundation with a higher groundwater level has a more serious uplift, which further causes larger ground vertical displacement. Fig. 10 illustrates the displacement vector of the overall site when the depth of the groundwater level is 1.6 m. It can be seen that the liquefied soil flows to the bottom of the station,

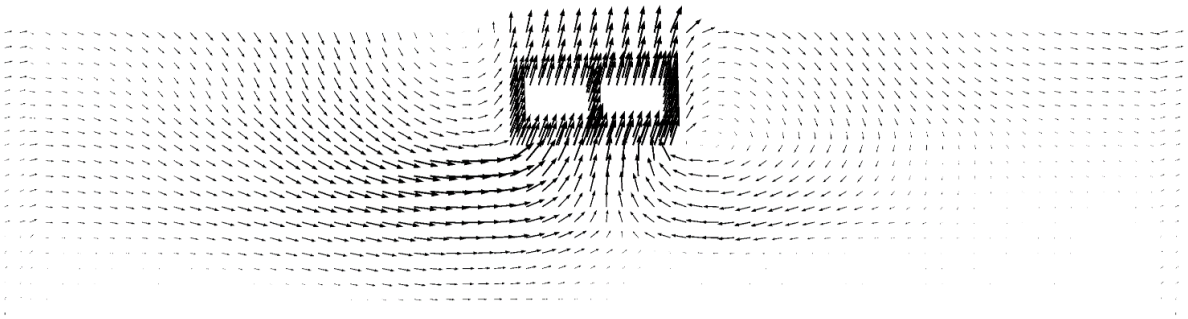

Fig. 10 Displacement vector of the overall site under PGA of 0.4 g

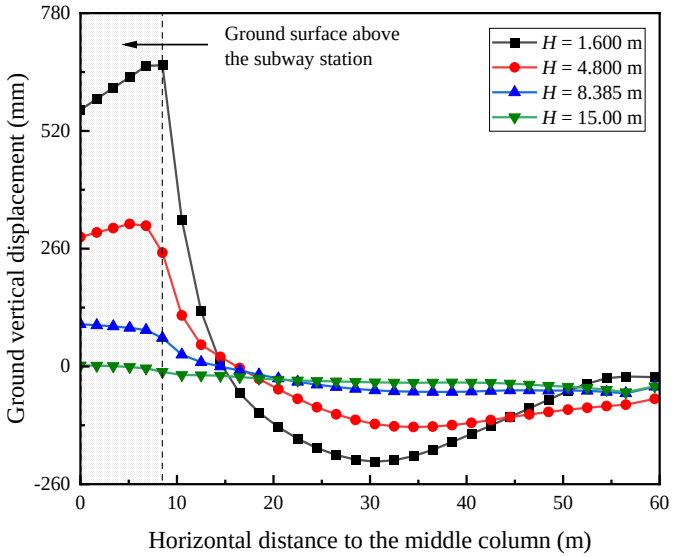

Fig. 11 Variation of ground vertical displacement with horizontal distance to the middle column for the input PGA of 0.4 g

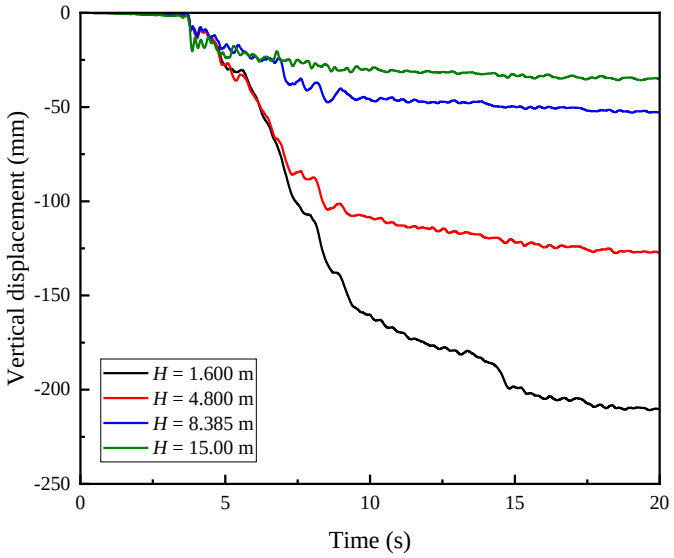

Fig. 12 Time-history curve of vertical displacement at measurement point 5 under PGA = 0.4 g

which intensifies the uplift behavior of the underground station. The variation of ground vertical displacement with horizontal distance to the station column during the earthquake with PGA = 0.4 g are presented in Fig. 11.

When PGA = 0.4 g, the peak ground vertical displacements are 665.02 mm, 314.37 mm, 93.02 mm and 2.21 mm respectively under four different depths of groundwater level from 1.6 m to 15 m. The decrease of

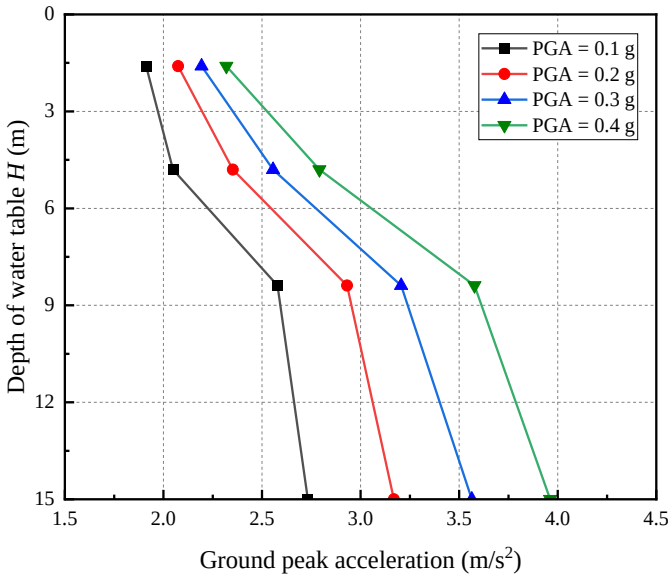

Fig. 13 Variation of peak ground acceleration with depth of the water table under different input PGAs

groundwater level greatly reduces the ground vertical displacement above the subway station after the earthquake.

To further illustrate the ground subsidence, Fig. 12 illustrates the time history of vertical displacement at measurement point 5. It can be stated that the seismic subsidence of the ground next to the underground station decreases with the decrease of groundwater level. After the earthquake, the final settlements are 210.15 mm, 127.20 mm, 52.68 mm and 35.30 mm respectively as the depth of the groundwater level rises from 1.6 m to 15 m. The final settlement at H = 1.6 m is about 6 times that at H = 15 m. It can be illustrated that the ground subsidence is significantly affected by the groundwater level.

3.3 Ground acceleration response

The variation of peak ground acceleration with the depth of the water table at measurement point 1 under different PGAs are presented in Fig. 13. Obviously, the peak ground acceleration rises as the depth of the water table increases. The development tendency of the ground peak acceleration is approximately consistent under different PGAs. When the input PGAs are 0.1 g, 0.2 g, 0.3 g and 0.4 g, the ground peak acceleration at H = 15 m is 42.85%, 52.78%, 62.48% and 70.79% larger than that at H = 1.6 m, respectively. It can be concluded that the variation amplitude of the peak ground acceleration rises with the increment of seismic intensity. The reason could be that when the groundwater level is relatively high, the liquefaction of the site is more serious under strong earthquakes, which leads to the stronger seismic isolation of the liquefied soils.

3.4 Dynamic soil pressure

To explore the influence of the different groundwater levels on dynamic soil pressure near the sidewall of the underground station, the variations of dynamic soil pressure with time at measurement points 2 and 3 are presented in Fig. 14. The buried depth of measurement point 2 is between 4.8 m and 8.385 m. Therefore, when the depths of the water table are 8.385 m and 15 m, measurement point 2 is above the groundwater level. Similarly, the measurement point 3 is above the groundwater level when H = 15. The results reveal that the variation amplitude of dynamic soil pressure below the water table is larger than that above the water table during earthquakes. The dynamic soil pressure decreases smoothly from 0 s to 3.4 s and then fluctuates after 3.4 s. In general, the dynamic soil pressure next to the sidewall of the underground station increases with the increment of seismic intensity. Meanwhile, the dynamic soil pressure decreases with the decrease of the groundwater level under the same input PGA. Therefore, there are apparent differences in dynamic soil pressure response near the sidewall under different groundwater levels, which could be adopted in the structural seismic design.

4. Numerical results and analysis for the structure

4.1 Structural displacement response

Fig. 15 indicates the variations of vertical displacement at the central point of the ceiling slab of the subway station with time subject to earthquakes with different seismic intensities. The general development tendencies of the vertical displacements of the station are approximately identical, while the differences in the displacement amplitude are significant under different depths of the water table. The development tendency of the vertical displacement can be divided into three stages. Specifically, the displacement curve drops slowly from 0 s to 3.4 s, while it fluctuates dramatically from 3.4 s to 10 s. Finally, the advance of the vertical displacement slows down and the curve develops smoothly after 10 seconds. Under PGA = 0.1 g, the station structure mainly reflects the state of settlement due to the low degree of site liquefaction, as seen

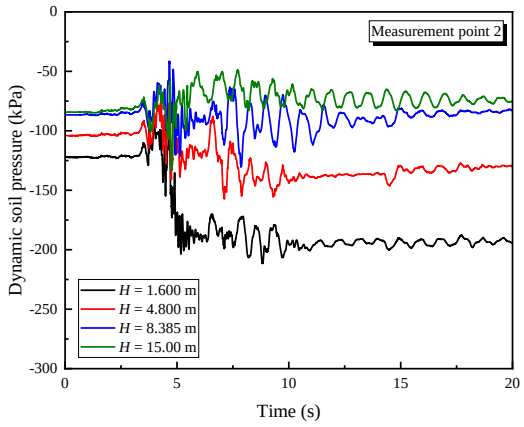

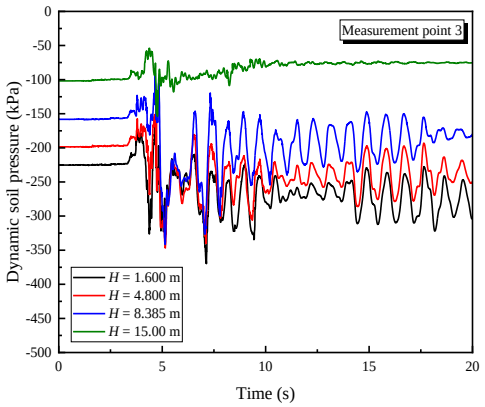

(a) PGA = 0.1 g

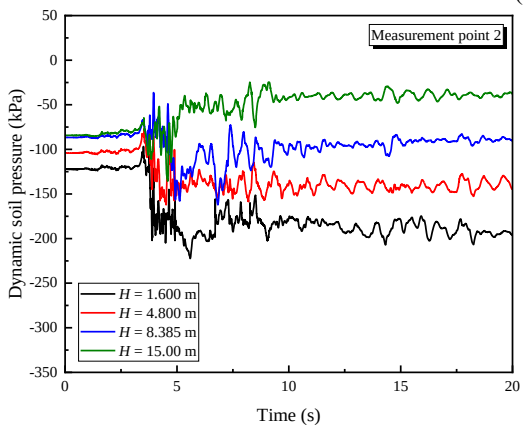

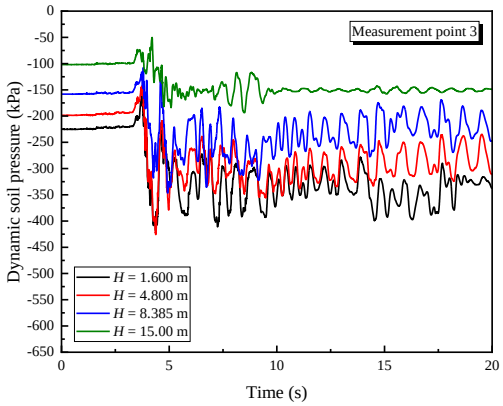

(b) PGA = 0.2 g

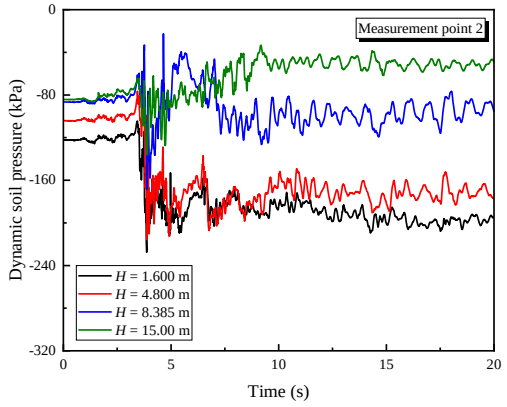

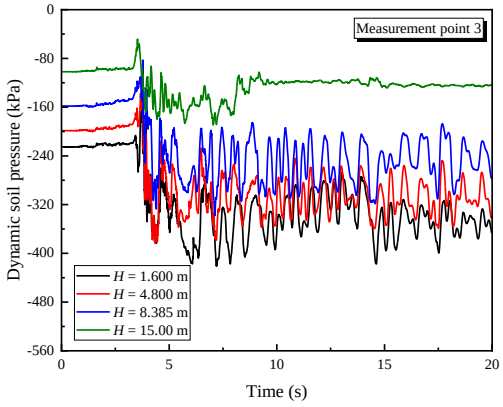

(c) PGA = 0.3 g

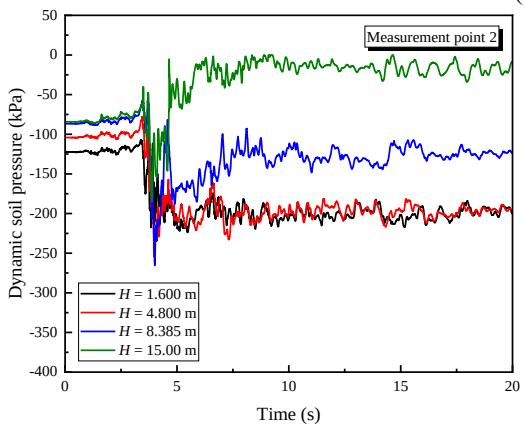

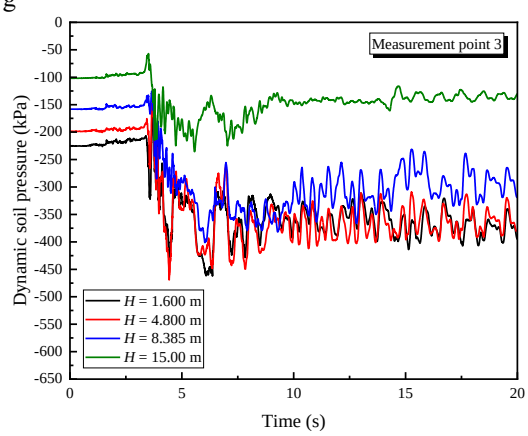

(d) PGA = 0.4 g

Fig. 14 Time-history curves of dynamic soil pressure near the sidewall under different PGAs

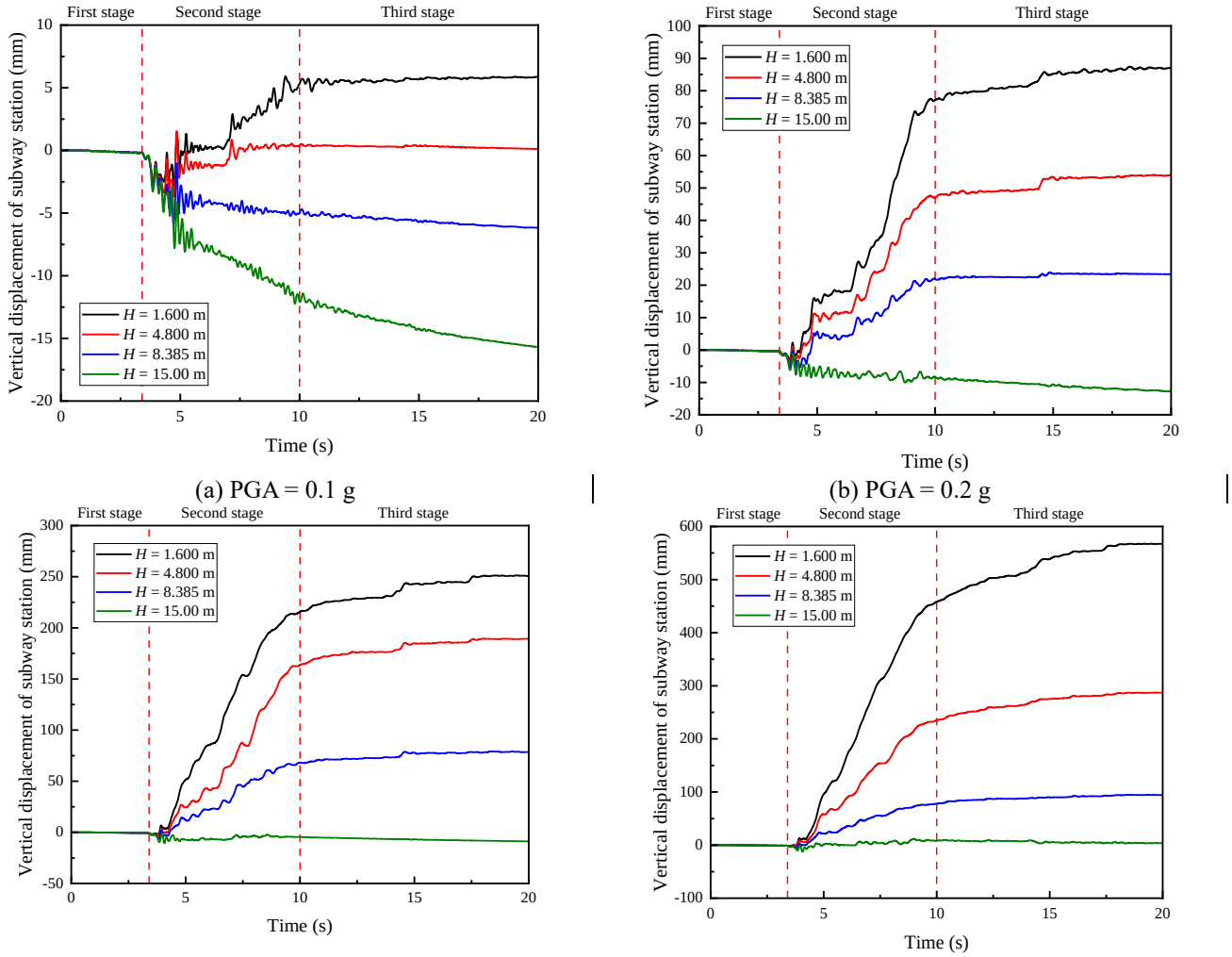

(a) PGA = 0.1 g (b) PGA = 0.2 g

(c) PGA = 0.3 g (d) PGA = 0.4 g

Fig. 15 Variations of vertical displacement of the subway station with time under different seismic intensities

in Fig. 15(a). After the earthquake, the final vertical displacements are 5.86 mm, 0.12 mm, -6.18 mm and -15.70 mm respectively with the *H* increasing from 1.6 m to 15 m. When the *H* is 1.6 m and 4.8 m, there is a slight uplift behavior for the subway station after the earthquake. The final displacement gradually reduces with the decrease of the groundwater level. When subject to the PGA of 0.2 g, compared to the PGA of 0.1 g, the higher liquefaction degree of the surrounding soil results in the more serious uplift behavior of the underground station, as seen in Fig. 15(b). After the earthquake, the final vertical displacements are 87.02 mm, 53.91 mm, 23.36 mm and -12.72 mm respectively with the *H* increasing from 1.6 m to 15 m. The results demonstrate that the subway station buried in the sand foundation with a higher groundwater level is more likely to uplift than that with a low groundwater level. The conclusion is also true when the PGAs are 0.3 g and 0.4 g, as illustrated in Figs. 15(c) and 15(d).

Fig. 16 shows the variations of horizontal displacement of the station structure with time subject to different input PGAs. When subject to PGA = 0.1 g, the curves of horizontal displacement fluctuate back and forth around the zero scale. The horizontal displacement is weakly influenced by the groundwater level. However, there is a large residual displacement of the underground station as the PGA rises from 0.2 g to 0.4 g. Besides, it can be concluded from the curves that the difference in the residual displacements is obvious under different groundwater levels. The reasons for the residual displacement of the subway station could be attributed to the unrecoverable deformation of the foundation after liquefaction during strong earthquakes. Similar unrecoverable lateral deformation of liquefied ground was also observed in a previous study (Zhuang *et al.* 2015b)

4.2 Structural stress response

The column is the weakest part of the Daikai station during an earthquake. The destruction of the station column led to the complete damage of the Daikai station in the Great Hanshin earthquake. Therefore, the axial stress and shear stress of the middle column are discussed and analyzed in this paper. Fig. 17 shows the measurement point layout of the station column. The peak axial stress of the station column subject to different PGAs is shown in Fig. 18. In general, the groundwater level has little influence on

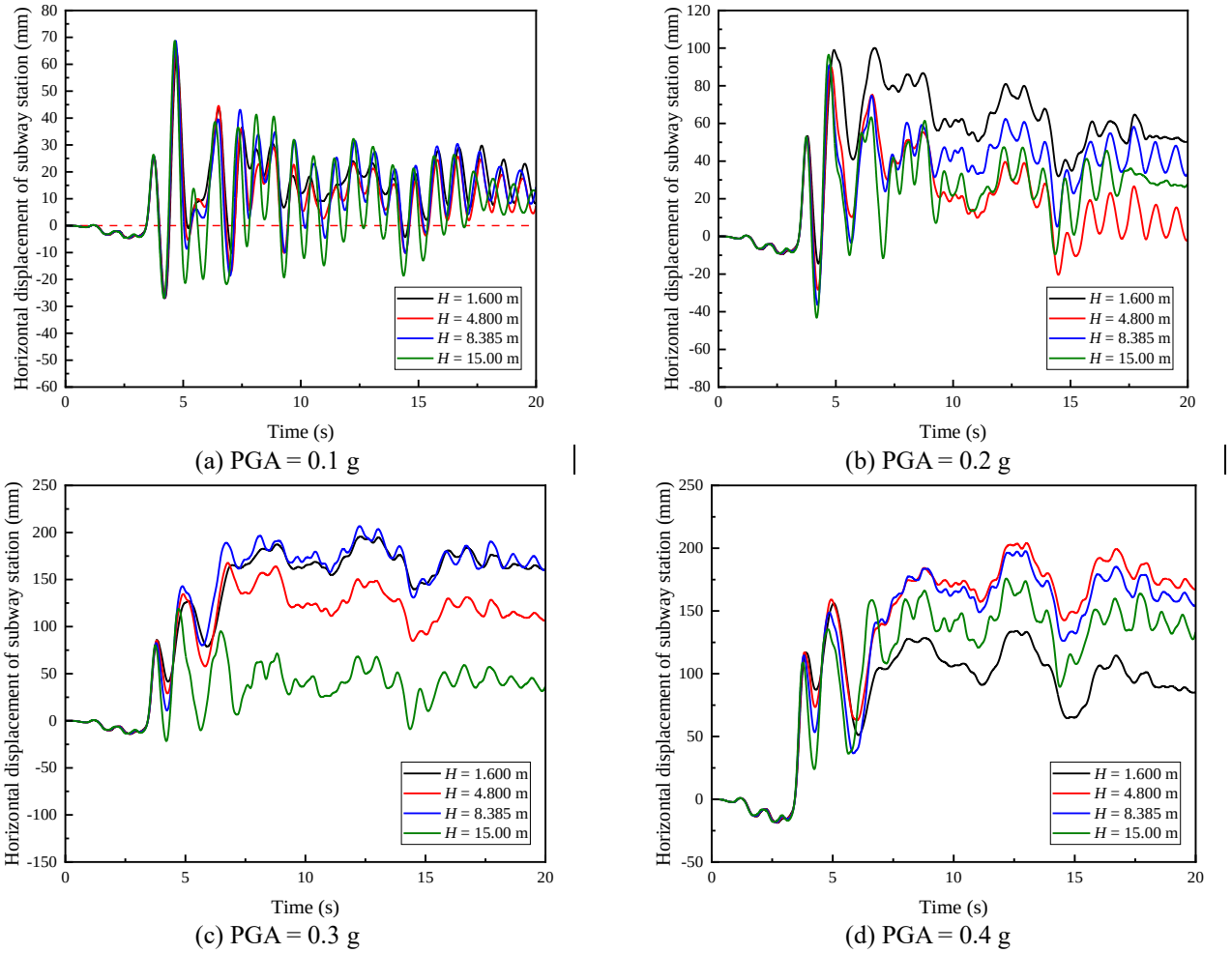

(a) PGA = 0.1 g (b) PGA = 0.2 g

(c) PGA = 0.3 g (d) PGA = 0.4 g

Fig. 16 Variations of horizontal displacement of the subway station with time under different seismic intensities

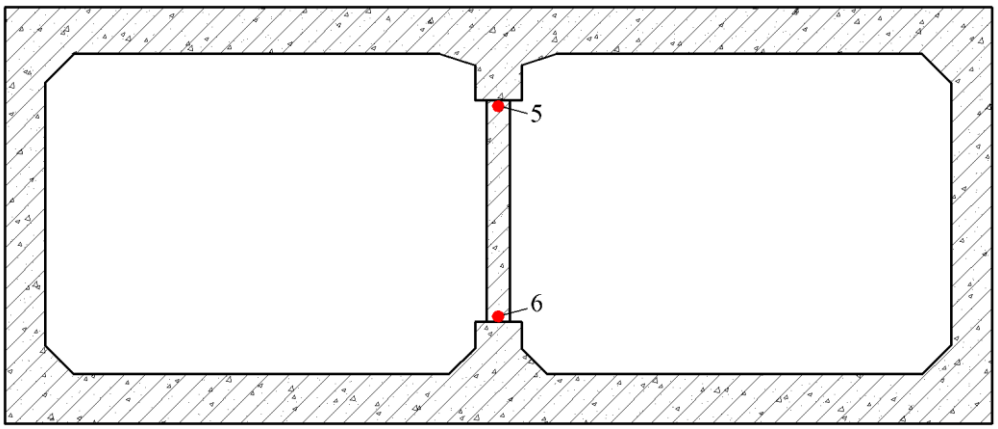

Fig. 17 Measurement points of the column

the peak axial stress of the middle column. The peak axial stress at the upper end of the middle column is generally consistent with that at the lower end of the middle column. The peak axial stress decreases first and then increases as the groundwater level decreases. The peak axial stress is the largest among the four different groundwater levels when the depth of the water table is 15 m, which is unfavorable to the compressive resistance of the station column.

Fig. 19 illustrates the peak shear stress of the middle column under different PGAs. The peak shear stress in the upper part of the station column is generally consistent with that in the lower part of the station column. When the depths of the water table are 1.6 m and 4.8 m, the peak shear stress increases as the PGA rises from 0.1 g to 0.3 g and then decreases when PGA = 0.4 g. The reduction of the peak shear stress could be attributed to the seismic isolation

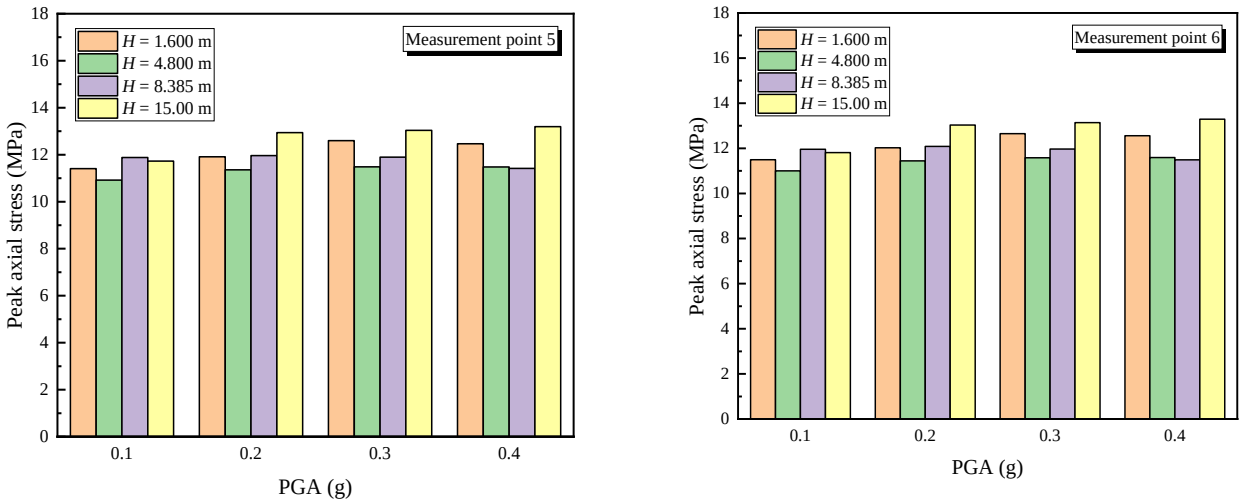

(a) Upper end of the column (b) Lower end of the column

Fig. 18 Peak axial stress of middle column under different seismic intensities

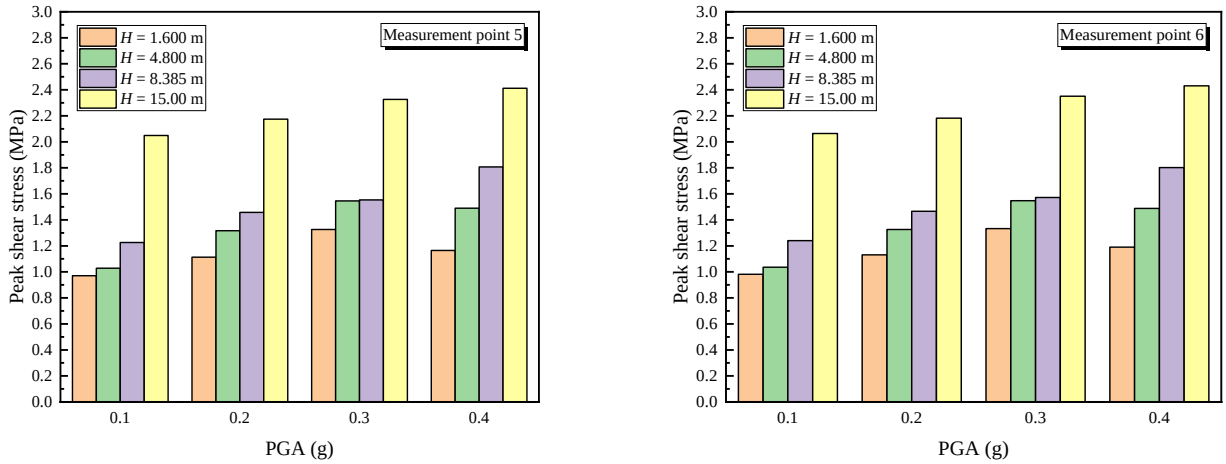

(a) Upper end of the column (b) Lower end of the column

Fig. 19 Peak shear stress of middle column under different PGAs

of the liquefied soils around the station under strong earthquakes. However, the decrease of groundwater level can significantly reduce the liquefaction scope of the foundation next to the station structure, as concluded in Section 3.1. Therefore, when the H is 8.385 m and 15 m, the peak shear stress rises as the PGA increases even under the PGA of 0.4 g. Moreover, the peak shear stress rises as the depth of the water table increases. For the upper end of the middle column, when PGA = 0.1 g, as the H rises from 1.6 m to 15 m, the peak shear stress is 0.97 MPa, 1.03 MPa, 1.23 MPa and 2.05 MPa, respectively. It can be concluded from the results that the decrease of groundwater level is unfavorable to the shear resistance of the station column. The conclusion is also true for other seismic intensities.

5. Conclusions

In this paper, the seismic response of the subway station buried in the sand foundation with different groundwater levels was studied by numerical analyses. The results indicate that the groundwater level has a great impact on the site liquefaction, ground displacement, dynamic soil pressure, ground acceleration and structural stress during and after earthquakes. The effects of different groundwater levels should be taken into account in the design of underground structures. The main conclusions are summarized as follows.

(1) There is no obvious site liquefaction around the sidewalls of the station. The underground station can constrain the liquefaction of the surrounding soil. The decrease of groundwater level can significantly reduce the liquefaction range of the foundation next to the station structure. Compared to other locations of the site, the foundation beneath the subway station is more likely to liquefy due to the uplift behavior of the underground station. The EPWP of the soil below the underground station becomes stronger as the water table becomes deeper. However, the EPWP ratio increases first and then decreases as the groundwater level declines because of the increment of the vertical initial effective stress.

(2) The area of ground settlement near the station reduces gradually with the decrease of groundwater level. The liquefied soil flow to the bottom of the station intensifies the uplift

behavior of the subway station. The decrease of the groundwater level significantly reduces the ground vertical displacement above the underground station after earthquakes.

(3) The seismic response of dynamic soil pressure below the water table is stronger than that above the water table during earthquakes. The dynamic soil pressure near the sidewall of the underground station increases as the seismic intensity increases. When subject to the same input PGA, the dynamic soil pressure with a higher water table is larger than that with a low water table. In addition, the ground peak acceleration increases as the groundwater level decreases under earthquakes.

(4) The development process of vertical displacement of the underground station is divided into three stages during an earthquake, including slow decline, dramatic fluctuation and smooth development. The subway station buried in the sand foundation with a higher groundwater level is more likely to uplift than that with a relatively low groundwater level under earthquakes. There is a large residual horizontal displacement of the subway station after strong earthquakes.

(5) The impact of different groundwater levels on the peak axial stress of the middle column can be ignored. With the decrease of groundwater level, the peak axial stress of the middle column decreases first and then increases. The decrease of groundwater level is unfavorable to the shear resistance of the station column. The peak shear stress rises as the depth of the groundwater level increases. When the groundwater level is relatively low, the peak shear stress rises as the PGA increases. However, the peak shear stress of the station column decreases with PGA = 0.4 g when the groundwater level is relatively high.

Acknowledgments

The work presented in this paper was funded by the National Natural Science Foundation of China (Grant No. 52378381), the Postgraduate Research & Practice Innovation Program of Jiangsu Province (Grant No. SJCX24_1462), the Graduate Innovation Program of China University of Mining and Technology (Grant No. 2024WLJCRCZL065) and China University of Mining and Technology (CUMT) Open Sharing Fund for Large-scale Instruments and Equipment (Grant No. DYGX-2024-43).

References

An, J.H., Tao, L.J., Jiang, L.Z. and Yan, H.J. (2021), "A shaking table-based experimental study of seismic response of shield-enlarge-dig type's underground subway station in liquefiable ground", *Soil Dyn. Earthq. Eng.*, **147**, 106621. https://doi.org/10.1016/j.soildyn.2021.106621.

Azadi, M. and Hosseini, S.M.M.M. (2010), "Analyses of the effect of seismic behavior of shallow tunnels in liquefiable grounds", *Tunn. Undergr. Sp. Tech.*, **25**(5), 543-552. https://doi.org/10.1016/j.tust.2010.03.003.

Bobet, A., Fernandez, G., Huo, H.B. and Ramirez, J. (2008), "A practical iterative procedure to estimate seismic-induced deformations of shallow rectangular structures", *Can. Geotech. J.*, **45**(7), 923-938. https://doi.org/10.1139/t08-026.

Chen, G., Chen, S., Qi, C., Du, X., Wang, Z. and Chen, W. (2014), "Shaking table tests on a three-arch type subway station structure in a liquefiable soil", *Bull. Earthq. Eng.*, **13**(6), 1675-1701. https://doi.org/10.1007/s10518-014-9675-0.

Cheng, X.L. and Sun, Z.G. (2018), "Effects of Burial Depth on the Seismic Response of Subway Station Structure Embedded in Saturated Soft Soil", *Adv. Civil Eng.*, 1-12. https://doi.org/10.1155/2018/8978467.

Chou, J.C. and Lin, E.G.E. (2020), "Incorporating ground motion effects into Sasaki and Tamura prediction equations of liquefaction-induced uplift of underground structures", *Geomech. Eng.*, **22**(1), 25-33. https://doi.org/10.12989/gae.2020.22.1.025.

Cui, Z.D., Zhang, L.J. and Hou, C.Y. (2023a), "Seismic behavior of subway station in the soft clay field before and after freeze-thaw cycle", *Soil Dyn. Earthq. Eng.*, **175**, 108222. https://doi.org/10.1016/j.soildyn.2023.108222.

Cui, Z.D., Zhang, L.J. and Zhan, Z.X. (2023b), "Seismic response analysis of shallowly buried subway station in inhomogeneous clay site", *Soil Dyn. Earthq. Eng.*, **171**, 107986. https://doi.org/10.1016/j.soildyn.2023.107986.

Ding, X., Zhang, Y., Wu, Q., Chen, Z. and Wang, C. (2021), "Shaking table tests on the seismic responses of underground structures in coral sand", *Tunn. Undergr. Sp. Tech.*, **109**, 103775. https://doi.org/10.1016/j.tust.2020.103775.

Dong, R., Jing, L., Li, Y., Yin, Z., Wang, G. and Xu, K. (2020), "Seismic deformation mode transformation of rectangular underground structure caused by component failure", *Tunn. Undergr. Sp. Tech.*, **98**, 103298. https://doi.org/10.1016/j.tust.2020.103298.

Ebadi-Jamkhaneh, M., Homaioon-Ebrahimi, A., Kontoni, D.P.N. and Shokri-Amiri, M. (2021), "Numerical FEM assessment of soil-pile system in liquefiable soil under earthquake loading including soil-pile interaction", *Geomech. Eng.*, **27**(5), 465-479. https://doi.org/10.12989/gae.2021.27.5.465.

Hamada, M., Towhata, I., Yasuda, S. and Isoyama, R. (1987), "Study on permanent ground displacement induced by seismic liquefaction", *Comput. Geotech.*, **4**(4), 197-220. https://doi.org/10.1016/0266-352X(87)90001-2.

Hashash, Y.M.A., Hook, J.J., Schmidt, B. and Yao, J.I.C. (2001), "Seismic design and analysis of underground structures", *Tunn. Undergr. Sp. Tech.*, **16**(4), 247-293. https://doi.org/10.1016/S0886-7798(01)00051-7.

Huo, H., Bobet, A., Fernández, G. and Ramírez, J. (2005), "Load transfer mechanisms between underground structure and surrounding ground:: Evaluation of the failure of the Daikai Station", *J. Geotech. Geoenviron. Eng.*, **131**(12), 1522-1533. https://doi.org/10.1061/(Asce)1090-0241(2005)131:12(1522).

Iida, H., Hiroto, T., Yoshida, N. and Iwafuji, M. (1996), "Damage to Daikai Subway Station", *Soils Found.*, **36**, 283-300. https://doi.org/10.3208/sandf.36.Special_283.

Jaber, L., Mezeh, R., Zein, Z., Azab, M. and Sadek, M. (2023), "Nonlinear numerical analysis of influence of pile inclination on the seismic response of soil-pile-structure system", *Geomech. Eng.*, **34**(4), 437-447. https://doi.org/10.12989/gae.2023.34.4.437.

Kang, G.C., Tobita, T. and Iai, S. (2014), "Seismic simulation of liquefaction-induced uplift behavior of a hollow cylinder structure buried in shallow ground", *Soil Dyn. Earthq. Eng.*, **64**, 85-94. https://doi.org/10.1016/j.soildyn.2014.05.006.

Koseki, J., Matsuo, O., Sasaki, T., Saito, K. and Yamashita, M. (2000), "Damage to sewer pipes during the 1993 Kushiro-Oki and the 1994 Hokkaido-Toho-Oki earthquakes", *Soils Found.*, **40**(1), 99-111. https://doi.org/10.3208/sandf.40.99.

Kuhlemeyer, R.L. and Lysmer, J. (1973), "Finite element method accuracy for wave propagation problems", *J. Soil Mech. Found. Div.*, **99**(5), 421-427. https://doi.org/10.1061/JSFEAQ.0001885.

Kwon, S.Y., Yoo, M. and Hong, S. (2020), "Earthquake risk assessment of underground railway station by fragility analysis

based on numerical simulation", *Geomech. Eng.*, **21**(2), 143-152. https://doi.org/10.12989/gae.2020.21.2.143.

Lu, C.C. and Hwang, J.H. (2019), "Nonlinear collapse simulation of Daikai Subway in the 1995 Kobe earthquake: Necessity of dynamic analysis for a shallow tunnel", *Tunn. Undergr. Sp. Tech.*, **87**, 78-90. https://doi.org/10.1016/j.tust.2019.02.007.

Sudevan, P.B., Boominathan, A. and Banerjee, S. (2020), "Mitigation of liquefaction-induced uplift of underground structures by soil replacement methods", *Geomech. Eng.*, **23**(4), 365-379. https://doi.org/10.12989/gae.2020.23.4.365.

Sun, Q., Dias, D., Guo, X. and Li, P. (2019), "Numerical study on the effect of a subway station on the surface ground motion", *Comput. Geotech.*, **111**, 243-254. https://doi.org/10.1016/j.compgeo.2019.03.026.

Suzuki, T., Adachi, Y. and Tanaka, M. (2006), "Application of microtremor measurements to the estimation of earthquake ground motions in Kushiro city during the Kushiro-Oki earthquake of 15 january 1993", *Earthq. Eng. Struct. D.*, **24**(4), 595-613. https://doi.org/10.1002/eqe.4290240409.

Tokimatsu, K. and Asaka, Y. (1998), "Effects of liquefaction-induced ground displacements on pile performance in the 1995 Hyogoken-Nambu earthquake", *Soils Found.*, **38**, 163-177. https://doi.org/10.3208/sandf.38.Special_163.

Tsinidis, G. (2017), "Response characteristics of rectangular tunnels in soft soil subjected to transversal ground shaking", *Tunn. Undergr. Sp. Tech.*, **62**, 1-22. https://doi.org/10.1016/j.tust.2016.11.003.

Unutmaz, B. (2014), "3D liquefaction assessment of soils surrounding circular tunnels", *Tunn. Undergr. Sp. Tech.*, **40**, 85-94. https://doi.org/10.1016/j.tust.2013.09.006.

Wang, J.N., Ma, G.W., Zhuang, H.Y., Dou, Y.M. and Fu, J.S. (2019), "Influence of diaphragm wall on seismic responses of large unequal-span subway station in liquefiable soils", *Tunn. Undergr. Sp. Tech.*, **91**, 102988. https://doi.org/10.1016/j.tust.2019.05.018.

Wu, Q., Ding, X., Zhang, Y., Chen, Z. and Zhang, Y. (2021), "Numerical simulations on seismic response of soil-pile-superstructure in coral sand", *Ocean Eng.*, **239**, 109808. https://doi.org/10.1016/j.oceaneng.2021.109808.

Xu, M.Z., Cui, Z.D. and Yuan, L. (2024), "Effect of relative stiffness on seismic response of subway station buried in layered soft soil foundation", *Geomech. Eng.*, **36**(2), 167-181. https://doi.org/10.12989/gae.2024.36.2.167.

Yoo, M., Kwon, S.Y. and Hong, S. (2022), "Dynamic response evaluation of deep underground structures based on numerical simulation", *Geomech. Eng.*, **29**(3), 269-279. https://doi.org/10.12989/gae.2022.29.3.269.

Zhuang, H., Chen, G., Hu, Z. and Qi, C. (2015b), "Influence of soil liquefaction on the seismic response of a subway station in model tests", *Bull. Eng. Geol. Environ.*, **75**(3), 1169-1182. https://doi.org/10.1007/s10064-015-0777-y.

Zhuang, H.Y., Hu, Z.H., Wang, X.J. and Chen, G.X. (2015a), "Seismic responses of a large underground structure in liquefied soils by FEM numerical modelling", *Bull. Earthq. Eng.*, **13**(12), 3645-3668. https://doi.org/10.1007/s10518-015-9790-6.